Simulating Charged Pion Decay Modes

Anisha Kadri, CID: 00946872
10th December, 2015

Abstract

A simulation of charged pion decays, ($\pi^+ \longrightarrow \mu^+ + \nu_\mu$ and $\pi^+ \longrightarrow e^+ + \nu_e$) was conducted to design an experiment that could measure the branching ratio of its decay modes. Both decay modes were simulated, using a hypothesised value of the branching ratio; 1 electron created in 10^4 pion decays. Using data for pion decay at various energies, the optimal location for detection was found.

1 Introduction

Both of the charged pions π^+, π^- decay via the weak force, and have two possible decay modes. The most common decay mode of the pion is into a muon and neutrino. This decay mode was first discovered in 1936[1] when muons (called mu-mesons at the time) were mistaken for pions.

$$\pi^+ \longrightarrow \mu^+ + \nu_\mu \tag{1}$$

$$\pi^- \longrightarrow \mu^- + \overline{\nu}_\mu \tag{2}$$

The second decay mode is the decay of a charged pion into an electron and its neutrino. This process is much less frequent, and was only discovered in 1958 [2].

$$\pi^- \longrightarrow e^- + \overline{\nu}_e \tag{3}$$

$$\pi^+ \longrightarrow e^+ + \nu_e \tag{4}$$

Since charge of the particles is the only difference in the decay modes of π^+, π^- mesons, they will be referred to as the same.

2 Theory

Branching ratio occurs because both decay methods are not equally likely- the muon decay mode is much more frequent for pions than the electron decay. This happens as a result of mass difference between the leptons and spin conservation during the decay[3]. Calculations using the half-widths of electrons and muons predict the branching ratio to be $1.283x10^4$[3], so the experiment must be optimised to measure a value in this region. Our ability to detect the pion decays is dependant on several factors, the energy of the pion (and thus the lifetime in the lab frame), the size of out chamber and resolution of our detector. Furthermore, muons also have a very short mean lifetime and decay into electrons with much greater frequency than pions. Thus, the signal of the electrons produced by pion decays is greatly masked by the electrons produced by muon decay.

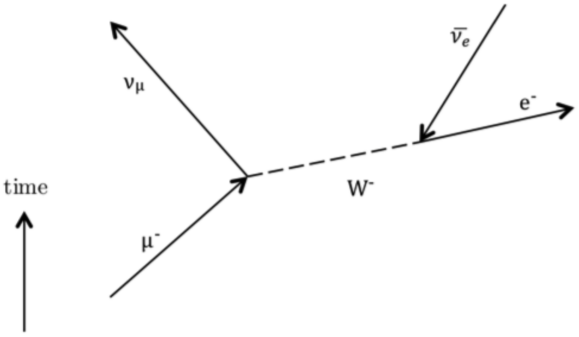

Figure 1: A Feynman diagram of a muon decaying into an electron via the weak force, also producing its neutrino and an electron neutrino. The direction of time is shown with an arrow.

2.1 Relativistic Relations and Four Vectors

Pions and muons have very short lifetimes, however when travelling at relativistic speeds the effect of time dilation allows them to be detectable in the lab frames.The relation between the decay time for a particle in its rest frame and the lab frame are related via the time dilation formula:

$$t = \gamma\tau \tag{5}$$

where t is the time measured in the lab frame and τ is the actual lifetime, or "proper time". Particles total energies and momentums can be represented in four-vector form. In natural units (where c=1), a four-vector is simplified to $(E, \underline{p})$ where the units of energy is eV, and momentum is in eVc^{-1}.

In their own rest frame, pions have no kinetic energy, and only rest mass energy. Energy conservation dictates the total energies (in the pion rest

frame) of the particles produced in a decay must be equal to the pion rest mass.

$$E_{e/\mu} = \frac{(m_\pi^2 + m_{e/\mu}^2 - m_\nu^2)}{2m_\pi} \tag{6}$$

However, neutrinos have negligible mass can be ignored to simplify the calculation. The particles momentums in the pion rest frame can also be calculated by the relativistic energy-momentum relation, which in natural units reduces to the following equation[5];

$$E_{total}^2 = p^2 + m^2 \tag{7}$$

where the units of energy are in eV, momentum are in eVc^{-1} and mass are eVc^{-2}. The energy momentum four-vector in the pion rest frame can then be boosted back into the lab frame by a Lorentz transformation, since we know the gamma factor for the pion that created the particle. In natural units;

$$\gamma = \frac{E_{total}}{m} \tag{8}$$

2.2 Particle Properties

A table of the values used for the particle properties [6];

Particle	Mass ($MeVc^{-2}$)	Mean Lifetime τ (s)
Pion, π	139.6	2.603×10^{-8}
Muon, μ	105.7	2.197×10^{-6}
Electron, e	0.5110	Stable

3 Method

3.1 Decay Chamber

The decay chamber simulated is a cylinder of radius 2.5m and length 100m. The Pion source is located at the origin of our defined co-ordinates system, and can produce pions in the range of 500- 10,000MeV. The response of an NaI scintillator detector is used in the simulation, with different amounts of energy deposited per cm for different particles.

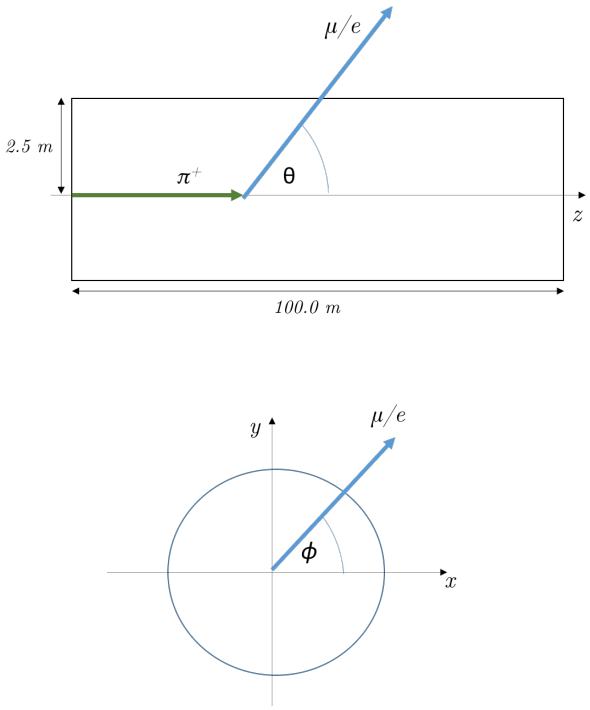

Figure 2: The cross- sectional views of the cylindrical decay chamber. The coordinates used in the method are as shown. The pions enter at the origin and travel in +z. The decay products are uniformly distributed in space.

3.2 Particle Classes

The particle base class allowed particles to be defined by their energy-momentum four vectors and the initial and final vertices of their paths. Their mass, gamma factor could be calculated. Derived classes of pions, muons and electrons inherit these methods. Pions were created with predetermined total energy within the source range. The magnitude of their momentum was calculated using the energy-momentum relation in Eq.7, and their direction was set as the +z direction (see Fig.2) to make the vector calculations more convenient.

3.3 Decay Methods

The decay time was calculated for pions and muons. Since the τ_π and τ_μ values in Section 2.2 are only mean lifetimes, the lifetimes of the pions and muons were found with a poisson distribution of τ. Using vectors, the time taken for the particle of given momentum to exit the chamber was also calculated.

The energy of muons and electrons produced by pions was calculated using Eq.6, but the electrons

produced by muons follow a Michel distribution. This was approximated by a triangular distribution with a peak energy of 53MeV.

Both the two body decays of the charged pion and the three body decay of the muon are simulated so that the direction of the charged daughter particle produced (i.e. the muon or electron) is distributed evenly in space. To simulate this a random number distribution in the interval $0 \leq \phi \leq 2\pi$ to find the azimuthal angle ϕ in Fig.2, and a random distribution for $\cos\theta$ in the interval $-1 \leq \cos\theta \leq 1$(since θ is the polar angle). The random decay of a pion into either an electron or a muon probability was simulated with binomial distribution of with a probability of an electron being $= 10^{-4}$.

4 Results

The final vertices of the particles' paths were plotted for various energies. The final positions were either where the particle left the chamber, or terminated via decay. The figures below show the exit positions of electrons created via the pion decay and muon decay respectively. Note that the number of final positions do not indicate frequency of decay modes, but rather the possible final positions of the decay products inside the chamber. The appendix contains scatter graphs for pion, muon and electron final positions for the energies 800MeV, 4900MeV and 9000MeV.

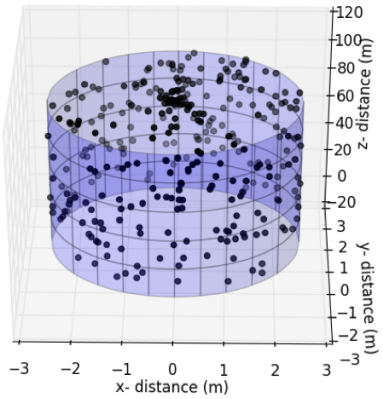

Figure 3: The final positions of electrons created by pion decay of 5000 source pions at 800MeV

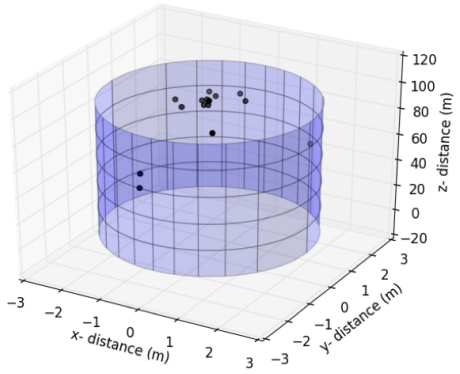

Figure 4: The final positions of electrons created by pion decay of 5000 source pions at 9000MeV

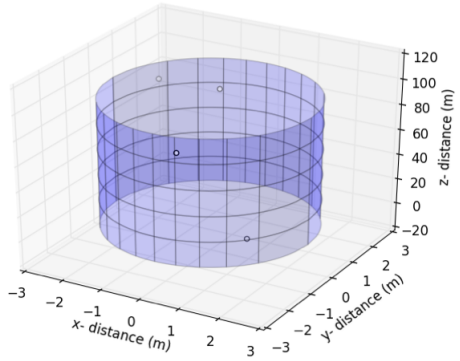

Figure 5: The final positions of electrons created by muon decay from 5000 source pions at 800MeV.

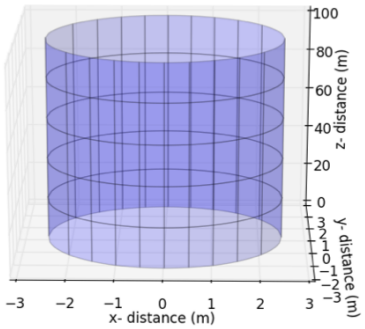

Figure 6: The final positions of electrons created by muon decay from 5000 source pions at 9000MeV..

The ratio of muons leaving/decaying in the chamber for different energies;

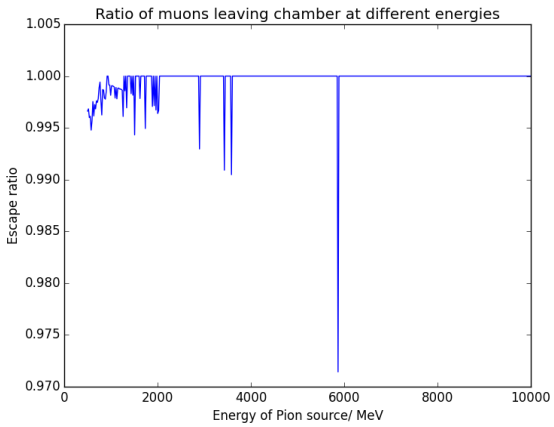

Figure 7: A graph showing the ratio of (muons leaving)/ (the total muons created)in the chamber and its variation with source energy.

4.1 Discussion of Results

The final vertices of particles created in the chamber can be seen in Fig.3 and Fig.4, which indicate that most muon and electron decays are detected with low energy pions between 500MeV- 1000MeV. This is because more energetic pions travel further, and are more likely to leave the chamber before decaying. For the same reason, it was found that the final positions of the daughter particles were concentrated nearer to the circular plane of the chamber (at z=100) for higher energies. They were more evenly distributed for lower energies.

Although less decays are detected on the whole for higher source energies, Fig.7 shows most muons escape before decaying into electrons. This means almost all the electron signals detected at high energies (between 6000MeV- 10,000MeV) are from the decay of pions. There is therefore less background from the muon decays when measuring the branching ratio.

4.2 Sources of Error and Limitations

There are many limitations of the pion decay simulation, due to assumptions made and computational capabilities. One such assumption was made when calculating the energies of the daughter particles of pion decays. The neutrino mass was neglected from Equation (6), assuming all the pions energy was converted into electrons/muons during the decay. Although the neutrino has a reasonably negligible rest mass in comparison to the other particles, it would still have some relativistic energy $E_\nu = pc$. This overestimate of total energy is a greater effect for the electron decay, as it is the lighter of the two daughter particles. For the simulation of the total energy of electrons produced by muon decay, a triangular distribution with a peak energy of 53MeV was used as an approximation of the Michel distribution. This is For the random decay of the pions, it was assumed that the branching ratio of the electron mode did not change as the total energy of the pion changed. There is a third decay mode of charged pions, the "pion beta decay " [7]mode (see Appendix), which also produces electrons, which has not been included in this simulation. However, this is a process even less frequent than the electron decay mode, and requires very high energy pions. For the energy range of the pion source simulated (500 -10000MeV), the contributions of the mode to the electron population is negligible.

5 Conclusion

It was found that the branching ratio could be better measured at higher energy source pions (> 6000MeV). This is because a greater proportion of muons escape before decaying. As a result, the percentage of electrons produced by pion decay is greater at high energies, and the background electrons from muon decay affects their measurement less. The optimal position for a detector to pick up the electrons produced by pions, is at face furthest from the The two body decay of the pions into muons and electrons could be better approximated by adding a E_ν term into the energy conservation. Rather than using the triangular distribution, a more accurate approximation of the Michel distribution result could be used by using the actual Michel parameters measured for muon decay.[8].

References

[1] Street JC, Stevenson EC. New evidence for the existence of a particle of mass intermediate between the proton and electron. Physical Review. 1937 Nov 1;52(9):1003.

[2] Fazzini, T.; Fidecaro, G.; Merrison, A.; Paul, H.; Tollestrup, A. (1958). "Electron Decay of the Pion". Physical Review Letters 1 (7): 247. doi:10.1103/PhysRevLett.1.247.

[3] Griffiths D. Introduction to Elementary Particles. John Wiley and Sons; 1987.

[4] Kadri A. Detecting Cosmic Rays Through Blackett Laboratory (First year Lab Report). 2015 Jun 18.

[5] Project B: Measuring Pi Decays. London: Imperial College London, Blackett Laboratory; 2015.

[6] Nakamura K, Particle Data Group. Review of particle physics. Journal of Physics G: Nuclear and Particle Physics. 2010 Jul 1;37(7A):075021.

[7] Bacastow R, Elioff T, Larsen R, Wiegand C, Ypsilantis T. Measurement of the Branching Ratio for Pion Beta Decay. Physical Review Letters. 1962 Nov 1;9(9):400.

[8] Jaros JA, Peskin ME. Nineteenth International Symposium on Lepton and Photon Interactions at High Energies. World Scientific; 2000.

6 Appendix

6.1 Pion Beta Decay

$$\pi^+ \longrightarrow \pi^0 + e^+ + \nu_e \tag{9}$$

6.2 More Final Mappings

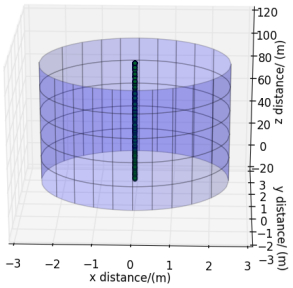

(a) The final positions of all 1000 source pions at 800MeV

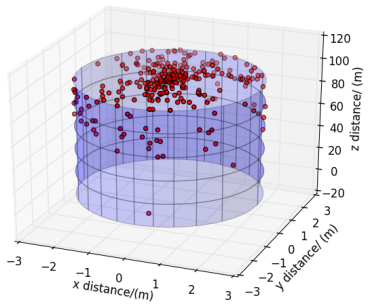

(b) The final positions of all muons created in the chamber by 1000 source pions at 800MeV

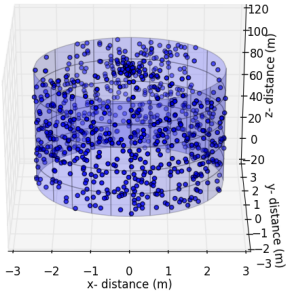

(c) The final positions of all electrons created in the chamber by 1000 source pions at 800MeV

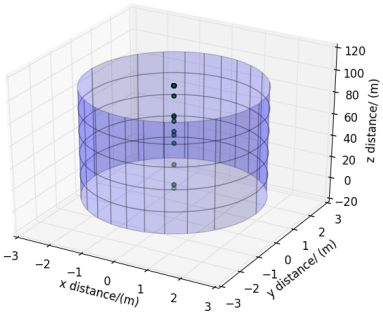

(d) The final positions of all 1000 source pions at 4900MeV

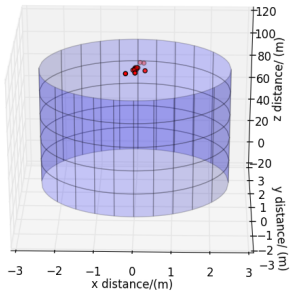

(e) The final positions of all muons created in the chamber by 1000 source pions at 4900MeV

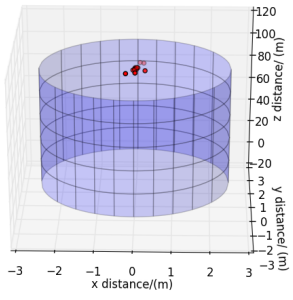

(f) The final positions of all electrons created in the chamber by 1000 source pions at 4900MeV